

# Shear induced breakup of droplets in a colloidal dispersion

Hideki Kobayashi<sup>1,2</sup> and Hiroshi Morita<sup>2</sup>

<sup>1</sup>*Theoretical Soft Matter and Biophysics, Institute of Complex Systems and Institute for Advanced Simulation, Forschungszentrum Juelich, 52425 Juelich, Germany and*

<sup>2</sup>*Soft Matter Modeling Group, Nanosystem Research Institute,*

*National Institute of Advanced Industrial Science and Technology, Umesono 1-1-1 Tsukuba 305-8568, Japan*

(Dated: September 13, 2021)

We present numerical results for the breakup of a pair of colloidal particles enveloped by a droplet under shear flow. The smoothed profile method is used to accurately account for the hydrodynamic interactions between particles due to the host fluid. We observe that the critical capillary number,  $Ca_B$ , at which droplets breakup depends on a velocity ratio,  $E$ , defined as the ratio of the boundary shift velocity (that restores the droplet shape to a sphere) to the diffusive flux velocity in units of the particle radius  $a$ . For  $E < 10$ ,  $Ca_B$  is independent of  $E$ , as is consistent with the regime studied by Taylor [1, 2]. When  $E > 10$ ,  $Ca_B$  behaves as  $Ca_B = 2E^{-1}$ , which confirms Karam and Bellinger's hypothesis [3]. As a consequence, droplet breakup will occur when the time scale of droplet deformation  $\dot{\gamma}^{-1}$  is smaller than the diffusive time scale  $t_D \equiv a^2/L\tau$  in units of  $a$ , where  $L$  is the diffusion constant and  $\tau$  is the 2nd order coefficient of the Ginzburg-Landau type free energy of the binary mixture. We emphasize that the breakup of droplet dispersed particles is not only governed by a balance of forces. We find that velocity competition is one of the important contributing factor.

PACS numbers: 47.55.D-, 47.55.df, 82.20.Wt, 82.70.Dd

A binary fluid system, such as a polymer blend, evolves under shear flow principally through the deformation and breakup of its constituent droplets [4]. Sheared binary fluids with dispersed colloidal particles are a topic of growing interest because they form the basis of many industrial products, for instance rubber products, plastic articles and some foods containing cornstarch or flour.

Breakup of Newtonian droplets suspended in a Newtonian fluid was studied and first understood by Taylor [1, 2]. He found, theoretically, in these purely viscous Newtonian systems that the deformation and breakup of droplets, in the absence of inertial forces, is governed by the capillary number  $Ca = \eta_c R \dot{\gamma} / \sigma$  and the viscosity ratio  $p = \eta_d / \eta_c$ , where  $\eta_c$  is the viscosity of the continuous phase,  $R$  is the droplet radius,  $\dot{\gamma}$  is the shear rate,  $\sigma$  is the interfacial tension and  $\eta_d$  is the viscosity of the droplet. The capillary number  $Ca = \eta_c R \dot{\gamma} / \sigma$  is the ratio of the viscous stress exerted on a droplet by shear flow to the interfacial tension that attempts to restore the droplet's shape to a sphere. When the viscous stress is larger than the interfacial tension, the droplet becomes unstable and breaks. The capillary number at which this breakup occurs is known as the critical capillary number,  $Ca_B$ . Taylor suggested that  $Ca_B$  is a function of  $p$ .

Taylor's result has been confirmed experimentally [3, 5–8] and numerically [9, 10]. In the experimental works [3, 5–8], the behavior of  $Ca_B$  is in reasonable quantitative agreement. According to these results,  $Ca_B$  exhibits a minimum in the range  $0.1 < p < 1$ . For  $1 < p$ , within the highly viscous regime,  $Ca_B$  increases with  $p$  until  $p \approx 4$ . For  $p > 4$ , droplet cannot be broken by shear. For  $0.01 < p < 0.1$ , where the viscosity  $\eta_d$  is low,  $Ca_B$  monotonically increases with decreasing  $p$ . In the highly

viscous regime, the rigidity of droplets increases with increasing  $p$  and finally the droplets behave almost like a rigid body. Thus, droplets cannot be broken by shear flow. In the low viscosity regime, Karam and Bellinger [3] hypothesized that  $Ca_B$ 's behavior derives from the shape of deformed droplets prior to breakup. They argued that a deformed droplet could be stabilized by the internally circulating fluid within it. Without internal circulation the deformed droplet is unstable and is likely to pinch off and divide due to interfacial tension. Internal circulation counteracts pinching-off by building the pressure against dimples, pushing them outwards. This behavior is typical of softmatter systems in which slow and fast dynamics coexist.

Evolution of the phase separation of binary fluid dispersed colloidal particles has been investigated by many researchers [11–17]. Introduction of colloidal particles strongly affects the phase structure. Neutral colloidal particles prefer to sit at the domain interface [11, 12]. When the volume fraction of colloidal particles is sufficiently large, domain growth stops when the interfacial region is filled with particles. As a result, the final phase structure is a gel [12]. Colloidal particles introduced into a binary fluid suppress the hydrodynamic flow induced by interface motion if particles favor one of the fluid phases. As a result, phase separation slows down [13–16]. With high concentrations of colloidal particles, attractive interactions, called wetting-induced depletion interactions, act between particles and thus the final structure becomes a network of particles connected by one phase [17].

Droplets of a colloidal dispersion under shear have been investigated experimentally [18, 19] and numerically [20, 21]. Inertia of the particles adsorbed to the droplet

interface causes the droplets to deform more strongly. As a result, droplets breakup more easily and  $Ca_B$  decreases in comparison to a Newtonian droplet [20]. In two dimensional simulations with low particle concentrations, the presence of dispersed particles or enveloped polymers serves to reduce the deformation of the droplet at intermediate  $Ca$ . However, long polymers induce droplet breakup at high  $Ca$  [21]. The mechanisms governing the breakup of droplets in the presence of dispersed particles are complex and have not been revealed completely until now.

In a droplet of a binary fluid dispersed colloid under shear, internal circulation is strongly affected by the impermeable surface of the colloidal particles. We hypothesize that the presence of particles suppresses the diffusive flux within the droplet. This effect leads to droplet instability. We analyze this effect and discover a new mechanism that governs droplet breakup. To accomplish this, we have devised a new methodology to directly simulate colloidal dispersions in a sheared binary fluid based on the smoothed profile method [22, 23].

We extend the smoothed profile method [22, 23] for the dynamics of colloidal dispersions in Newtonian fluids to sheared binary fluids. In this method, boundaries between solid particles and solvents are replaced with a continuous interface by assuming a smoothed profile. This enables us to calculate the hydrodynamic interactions both efficiently and accurately, without neglecting many-body interactions.

We employ the following free energy functional for a binary mixture containing particles:

$$F\{\psi, \phi\} = \int d\mathbf{r} \{f(\psi) - W\psi|\nabla\phi|^2 - \chi(\Delta\psi)^2\phi\}, \quad (1)$$

where  $\psi$  is a concentration field and  $\phi$  is a smoothed profile function. The smoothed profile function  $0 \leq \phi(\mathbf{r}, t) \leq 1$  distinguishes between the fluid and particle domains, with  $\phi = 1$  in the particle domain and  $\phi = 0$  in the fluid domain. These domains are separated by thin interfacial regions with a thickness characterized by  $\xi$ . The first term on the right-hand side of equation (1) corresponds to a Ginzburg-Landau type mixing free energy for a binary fluid:  $f(\psi) = -\tau\psi^2/2 + u\psi^4/4 + K|\nabla\psi|^2/2$ , where  $\tau, \mu$  and  $K$  are constants. The second term represents the wetting interaction between the binary fluid and the particle surface, which is represented by  $|\nabla\psi|^2$ .  $W$  expresses the strength of the wetting interaction. With  $W > 0$  ( $W < 0$ ), the phase with  $\psi > 0$  ( $\psi < 0$ ) favours the particle surface. The third term is introduced so that the concentration field inside each particle favors a surface phase.  $\chi$  is the coupling constant and  $\Delta\psi = \psi - W/|W|$  ( $W \neq 0$ ),  $\psi$  ( $W = 0$ ).

The time dependence of the concentration field  $\psi$  and the fluid velocity  $\mathbf{u}$  are given by

$$\frac{\partial\psi}{\partial t} = -(\mathbf{u} \cdot \nabla)\psi + L\nabla \cdot \{(I - \mathbf{n}\mathbf{n}) \cdot \nabla\mu\} \quad (2)$$

$$\rho_f \left\{ \frac{\partial\mathbf{u}}{\partial t} + (\mathbf{u} \cdot \nabla)\mathbf{u} \right\} = -\psi\nabla\mu - \nabla p + \eta\nabla^2\mathbf{u} + \rho_f\phi\mathbf{f}_p + \mathbf{f}_{\text{shear}} \quad (3)$$

under the incompressibility condition  $\nabla \cdot \mathbf{u} = 0$ , where  $\mu$  is  $\delta F/\delta\psi$ ,  $I$  is the unit tensor,  $\mathbf{n}$  is a unit vector field defined by  $-\nabla\phi/|\nabla\phi|$  and  $\rho_f, \eta, L$  and  $p(\mathbf{r}, t)$  are the density, shear viscosity, diffusion constant and pressure field of the solvent, respectively. The operator  $(I - \mathbf{n}\mathbf{n})$  directly assigns the no-penetration condition at interfacial regions. Note that, in this paper, we assume that the two phases have the same viscosity and thus the viscosity ratio  $p = 1$ . A body force  $\phi\mathbf{f}_p$  is introduced to ensure rigidity of the particles and to enforce non-slip boundary conditions at the fluid/particle interface. Mathematical expressions for  $\phi$  and  $\phi\mathbf{f}_p$  are detailed in previous papers [22, 23]. The external force  $\mathbf{f}_{\text{shear}}$  is introduced to maintain a linear shear with shear rate  $\dot{\gamma}$ . This force is applied using an oblique coordinate transformation based on tensor analysis [24, 25].

In the present study, we treat colloidal particles as beads of radius  $a$ . The motion of the  $i$ th bead is governed by Newton's and Euler's equations of motion with:

$$M_i \frac{d}{dt} \mathbf{V}_i = \mathbf{F}_i^H + \mathbf{F}_i^P, \quad \frac{d}{dt} \mathbf{R}_i = \mathbf{V}_i, \quad (4)$$

$$\mathbf{I}_i \cdot \frac{d}{dt} \boldsymbol{\Omega}_i = \mathbf{N}_i^H, \quad (5)$$

where  $\mathbf{R}_i, \mathbf{V}_i$  and  $\boldsymbol{\Omega}_i$  are the position, translational velocity, and rotational velocity of the beads, respectively.  $M_i$  and  $\mathbf{I}_i$  are the mass and moment of inertia, and  $\mathbf{F}_i^H$  and  $\mathbf{N}_i^H$  are the hydrodynamic force and torque exerted by the solvent on the beads, respectively [22, 23].  $\mathbf{F}_i^P$  represents the potential force due to direct inter-bead interactions, such as Coulombic or Lennard-Jones potentials. The truncated Lennard-Jones interaction is expressed in terms of  $U_{LJ}$ :

$$U_{LJ}(r_{ij}) = \begin{cases} 4\epsilon \left\{ \left( \frac{2a}{r_{ij}} \right)^{12} - \left( \frac{2a}{r_{ij}} \right)^6 \right\} + \epsilon & (r_{ij} < 2\frac{7}{6}a), \\ 0 & (r_{ij} > 2\frac{7}{6}a), \end{cases} \quad (6)$$

where  $r_{ij} = |\mathbf{R}_i - \mathbf{R}_j|$ . The parameter  $\epsilon$  characterizes the strength of the interactions.

Numerical simulations have been performed in three spatial dimensions with periodic boundary conditions. The lattice spacing  $\Delta$  is set to unit length. The phase interfacial length  $l = \sqrt{K/\tau} = 1$  or 2 and the interfacial tension  $\sigma = \sqrt{\tau K} = \tau l$ . The unit of time is

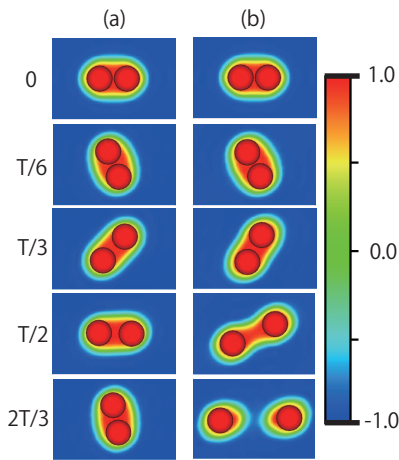


FIG. 1: Schematic illustration of the rotation and breakup of a droplet.  $T$  is the tumbling period. The legend relates the color to the concentration. (a)  $Ca$  is sufficiently small and the droplet can rotate. (b)  $Ca$  is sufficiently large and the droplet breaks up before it can tumble.

given by  $\rho_f \Delta^2 / \eta$ , where  $\eta = 1$  and  $\rho_f = 1$ . The system size is  $L_x \times L_y \times L_z = 64 \times 64 \times 32$ . The range of  $\dot{\gamma}$  is  $2.0 \times 10^{-3} < \dot{\gamma} < 4.0 \times 10^{-3}$  and that of  $L$  is  $8.0 \times 10^{-2} < L < 1.8$ . The remaining parameters are as follows:  $\tau = u = K/l^2 = 0.01 \sim 1.0$ ,  $\chi = 10W = 100l\eta\dot{\gamma}$ ,  $a = 4$  or  $5$ ,  $\xi = 2$ ,  $\epsilon = 1$ ,  $M_i = 4\pi a^3/3$  and  $h = 0.064$ , where  $h$  is the time increment of a single simulation step.

The initial state of the binary fluid is set according to the following procedure. At first, two particles are introduced at  $(32 - a, 32, 16)$  and  $(32 + a, 32, 16)$  into a homogeneous concentration of average concentration  $\bar{\psi} = -0.93$  and  $\tau = u = K = 0.1$ ,  $W = 0.04$ ,  $\chi = 0.4$ ,  $L = 1.6$ . We then iterate until steady state. Afterwards, we increment by a single time step.

In the following simulations, the time dependence of the concentration field  $\psi$  and the fluid velocity  $\mathbf{u}$  are discretized using a de-aliased Fourier spectral scheme in space and an Euler scheme in time. To follow bead motions, the position, velocity and angular velocity of the beads are integrated by the Adams-Bashforth scheme.

Fig. 1 is a schematic illustration of the rotation and breakup of a droplet. When the interfacial tension is sufficiently large, as in (a), the droplet undergoes a tumbling motion similar to a chain [26], although this tumbling has a limited lifetime. On the other hand, in (b), the interfacial tension is small and we expect the droplet to break-up before undergoing tumbling.

We define the breakup shear rate  $\dot{\gamma}_B$  as the shear rate at which a droplet of a colloidal dispersion becomes unable to tumble for a given  $\sigma$ . The break up capillary number  $Ca_B$  is defined as

$$Ca_B \equiv \frac{2\eta a \dot{\gamma}_B}{\sigma}, \quad (7)$$

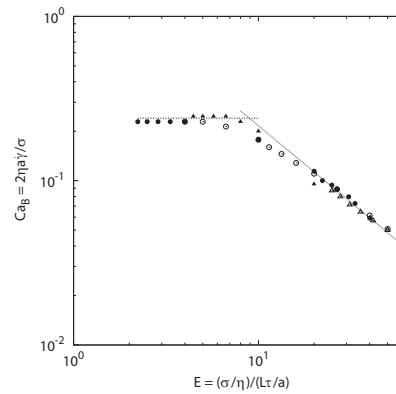


FIG. 2:  $Ca_B$  as a function of  $E$ . Closed circles ( $a = 4, \dot{\gamma} = 2.0 \times 10^{-3}, l = 1$ ). Open circles ( $a = 4, \dot{\gamma} = 4.0 \times 10^{-3}, l = 1$ ). Closed triangles ( $a = 4, \dot{\gamma} = 1.0 \times 10^{-3}, l = 2$ ). Open triangles ( $a = 5, \dot{\gamma} = 2.0 \times 10^{-3}, l = 1$ ). The dashed line corresponds to  $Ca_B = 0.24$ . The dotted line corresponds to  $Ca_B = 1.84E^{-0.931}$ .

assuming that the droplet radius is roughly estimated by  $2a$ .

To quantify the barrier to internal circulation due to the particles, we introduce the velocity ratio  $E$  which is a dimensionless number given by the ratio of the boundary shift velocity (that restores the droplet shape to a sphere) to the diffusive flux velocity in units of the particle radius  $a$ . Concretely speaking,  $E$  is expressed as

$$E \equiv \frac{\sigma/\eta}{L\tau/a} = \frac{la}{\eta L}. \quad (8)$$

We plot the behavior of  $Ca_B$  as a function of  $E$  in Fig. 2. Were droplet breakup driven purely by the mechanism described in earlier works [1–3, 5–9],  $Ca_B$  would be independent of  $E$ . For  $E < 10$ ,  $Ca_B$  is constant, namely  $Ca_B \approx 0.24$ . Previous works [1–3, 5–9] reported a critical capillary number of  $Ca_B \approx 0.5$  in the absence of particles and with equal droplet and solvent viscosities. Our value of  $Ca_B$  is smaller than the previously reported result due to the presence of colloidal particles near the interface.

We confirm that the mechanism governing the breakup of droplet dispersed colloids in this regime is the same mechanism as described in Taylor's works [1, 2]. According to Taylor's work [1], a critical capillary number  $Ca_B$  is estimated. We neglect the deviation of the droplet shape from a sphere. When the droplet radius is roughly approximated by  $2a$ , the maximum pressure difference across the interface is  $\delta p \approx 4\eta\dot{\gamma}$  and the Laplace pressure due to interfacial tension is  $\delta p_L = \sigma/a$ . The Stokes force exerted on the colloidal particles is estimated as  $6\pi\eta ad\dot{\gamma}$  where  $d$  is the distance between particles, approximated as  $d = 2a$ . Thus, the Stokes force per unit area,  $\delta F_S$ , is approximately  $6\pi\eta ad\dot{\gamma}/2\pi a^2 = 6\eta\dot{\gamma}$ . Assuming that the droplet breaks when  $\delta p + \delta F_S > \delta p_L$ , we can predict  $Ca_B \approx 0.2$ . This estimate is in good agreement with our

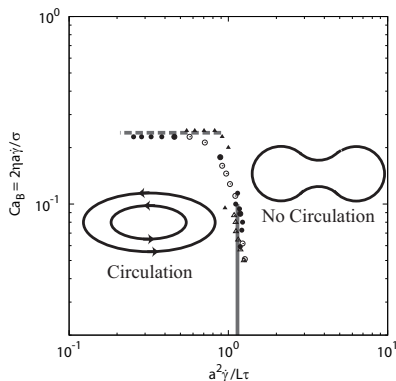


FIG. 3:  $Ca_B$  as a function of  $a^2\dot{\gamma}/L\tau$ . Closed circles ( $a = 4, \dot{\gamma} = 2.0 \times 10^{-3}, l = 1$ ). Open circles ( $a = 4, \dot{\gamma} = 4.0 \times 10^{-3}, l = 1$ ). Closed triangles ( $a = 4, \dot{\gamma} = 1.0 \times 10^{-3}, l = 2$ ). Open triangles ( $a = 5, \dot{\gamma} = 2.0 \times 10^{-3}, l = 1$ ). The dashed line corresponds to  $Ca_B = 0.24$ . The solid line corresponds to  $a^2\dot{\gamma}/L\tau = 1.14$ .

result  $Ca_B \approx 0.24$ .

However, when  $E > 10$ ,  $Ca_B$  comes to depend on  $E$ . Although the interfacial tension exceeds the viscous stress, the droplet is broken by the shear flow in this regime. We reveal for the first time that  $Ca_B$  can be described by

$$Ca_B = 1.80E^{-0.93}. \quad (9)$$

This equation implies that  $Ca_B$  decreases with decreasing inner circulation due to the diffusion flux. This behavior confirms Karam and Bellinger's hypothesis [3].

Furthermore, Eq. (9) not only confirms Karam and Bellinger's hypothesis [3] but also demonstrates a new source of instability originating from the competition between shear flow and diffusive flux. For droplet dispersed colloidal particles, internal circulation, which corresponds to a phase diffusive flux, is obstructed by the particle surface. The phase diffusive flux takes some amount of time,  $t_D \equiv a^2/L\tau$ , to overcome this obstruction. When  $t_D$  is larger than the time scale of droplet deformation  $\dot{\gamma}^{-1}$ , droplets can break up even when interfacial tension exceeds the viscous stress. Therefore, we predict that the droplet is unstable when  $a^2\dot{\gamma}/L\tau > 1$ . On the basis of this, an instability condition can be derived as:

$$Ca > 2E^{-1}, \quad (10)$$

which is in good qualitative agreement with Eq. (9).

To verify the instability condition,  $Ca_B$  is plotted as a function of  $a^2\dot{\gamma}/L\tau$  in Fig. 3. Fig. 3 shows that the droplet is stable for both  $Ca < 0.24$  and  $a^2\dot{\gamma}/L\tau < 1.14$ . Although the interfacial tension exceeds the viscous stress, the droplet is unstable and breaks up when  $a^2\dot{\gamma}/L\tau > 1.14$ . This result is in good agreement with our prediction, thus validating our instability condition.

The breakup of pairs of colloidal particles enveloped by a droplet under shear flow was numerically calculated using the smoothed profile method extended to sheared binary fluids for  $4.0 \times 10^{-2} < Ca < 4.0 \times 10^{-1}$  and  $2.0 \times 10^{-1} < a^2\dot{\gamma}/L\tau < 2.0$ . Breakup occurs for  $0.24 < Ca$  and  $1.14 < a^2\dot{\gamma}/L\tau$ .

Droplet breakup at  $Ca \approx 0.24$  occurs because the viscous stress exceeds the interfacial tension.

At  $a^2\dot{\gamma}/L\tau \approx 1.14$  breakup occurs because the time scale of droplet deformation  $\dot{\gamma}^{-1}$  is smaller than  $t_D \equiv a^2/L\tau$ . We emphasize that this instability is not derived from force competition. It is driven by velocity competition.

- 
- [1] G. I. Taylor, Proc. Roy. Soc. **138A**, 41 (1932).
  - [2] G. I. Taylor, Proc. Roy. Soc. **146A**, 501 (1934).
  - [3] H. J. Karam and J. C. Bellinger, I. & EC. Fundamentals **7**, 576 (1968).
  - [4] K. B. Migler, Phys. Rev. Lett. **86**, 1023 (2001).
  - [5] F. D. Rumscheidt and S. G. Mason, J. Coll. Sci. **16**, 238 (1961).
  - [6] S. Torza, R. G. Cox, and S. G. Mason, J. Coll. Sci. **38**, 395 (1972).
  - [7] H. P. Grace, Chem. Eng. Commun. **14**, 225 (1982).
  - [8] P. P. Varanasi, M. E. Ryan, and P. Stroeve, Ind. Eng. Chem. Res. **33**, 1858 (1994).
  - [9] H. Xi and C. Duncan, Phys. Rev. E **59**, 3022 (1999).
  - [10] P. J. Janssen and P. D. Anderson, Phys. Fluids **19**, 043602 (2007).
  - [11] B. P. Binks and J. H. Clint, Langmuir **18**, 1270 (2002).
  - [12] K. Stanford, R. Adhikari, I. Pagonabarraga, J. C. Desplat, and M. E. Cates, Science **309**, 2198 (2005).
  - [13] F. Qiu, G. Peng, V. V. Ginzburg, A. C. Balaz, H. Y. Chen, and D. Jasnow, J. Chem. Phys. **115**, 3779 (2001).
  - [14] D. Suppa, O. Suksenok, A. C. Balaz, and J. M. Yeomans, J. Chem. Phys. **116**, 6305 (2002).
  - [15] M. Laradji and G. MacNevin, J. Chem. Phys. **119**, 2275 (2003).
  - [16] R. Verberg, J. M. Yeomans, and A. C. Balazs, J. Chem. Phys. **123**, 2005 (2005).
  - [17] T. Araki and H. Tanaka, Phys. Rev. E **73**, 061506 (2006).
  - [18] M. Desse, B. Wolf, J. Mitchell, and T. Budtova, J. Rheol. **53**, 943 (2009).
  - [19] M. Desse, D. Fraiseau, J. Mitchell, and T. Budtova, Soft Matter **6**, 363 (2010).
  - [20] S. Frijters, F. Guenther, and J. Harting, Soft Matter **8**, 6542 (2012).
  - [21] O. B. Usta, D. Perchak, A. Clarke, J. M. Yeomans, and A. C. Balazs, J. Chem. Phys. **130**, 234905 (2009).
  - [22] Y. Nakayama and R. Yamamoto, Phys. Rev. E **71**, 036707 (2005).
  - [23] Y. Nakayama, K. Kim, and R. Yamamoto, Eur. Phys. J. E **26**, 361 (2008).
  - [24] A. Onuki, J. Phys. Soc. Jpn. **66**, 1836 (1997).
  - [25] H. Kobayashi and R. Yamamoto, J. Chem. Phys. **134**, 064110 (2011).
  - [26] G. B. Jeffery, Proc. R. Soc. A **102**, 161 (1922).